

OXYGEN ISOTOPE RESERVOIRS IN THE PROTOPLANETARY DISK INFERRED FROM CHONDRULES IN PRIMITIVE METEORITES. N. T. Kita¹, T. J. Tenner², T. Ushikubo³, D. Nakashima⁴, C. Defouilloy¹, A. T. Hertwig¹, N. Chaumard¹, N. G. Rudraswami⁵, M. K. Weisberg^{6,7}, M. Kimura⁸, H. Nagahara⁹, and A. Bischoff¹⁰. ¹WiscSIMS, University of Wisconsin-Madison, Madison, WI 53706. (noriko@geology.wisc.edu). ²Los Alamos National Laboratory, Los Alamos, NM 87545. ³Kochi Institute for Core Sample Research, JAMSTEC, Kochi 783-8502, Japan. ⁴Tohoku University, Miyagi 980-8578, Japan. ⁵National Institute of Oceanography, Dona Paula, Goa 403004, India. ⁶Kingsborough College and Graduate Center, CUNY, Brooklyn, NY 11235. ⁷American Museum Natural History, New York, NY 10024. ⁸Ibaraki University, Mito 310-8512, Japan. ⁹University of Tokyo, Tokyo 113-0033, Japan, ¹⁰Institut für Planetologie, WWU Münster, 48149 Münster, Germany.

Introduction: The Solar System appears to have started with heterogeneous ¹⁶O abundances. Large variability in O 3-isotope ratios (¹⁷O/¹⁶O and ¹⁸O/¹⁶O ratios expressed as $\delta^{17}\text{O}$ and $\delta^{18}\text{O}$: relative to Standard Mean Ocean Water in the unit of 1/1000) are observed among the Sun ($\delta^{17}\text{O}$, $\delta^{18}\text{O}$ ~ -60‰ [1]), Ca,Al-rich inclusions (CAIs; -50‰ [2]) and cosmic symplectites (COS; +200‰ [3]). Chondrules in primitive chondrites show a smaller and intermediate range of $\delta^{17,18}\text{O}$, from -15‰ to +5‰ [e.g., 4]. According to ²⁶Al-²⁶Mg chronology, most chondrules formed 2-3 Myr after CAIs [5-6] in the dust-rich environments [7-8]. It is suggested that chondrule formation occurred in an open system with respect to oxygen by evaporation and recondensation processes [9] and oxygen in the ambient gas during chondrule formation would have been dominated by that from solid precursors [10-11]. If true, then the chondrule melt and ambient gas would have had similar O-isotope ratios as precursor dusts. Thus, O-isotope ratios of chondrules may reflect temporal and/or spatial varieties of such reservoirs in the protoplanetary disk.

We have conducted O 3-isotope analyses of ~600 chondrules from multiple chondrite groups (O, R, EH, CO, CV, CM, CR, CH, ungrouped C) using a secondary ion mass spectrometer (WiscSIMS) at sub-‰ precision [10-26]. For most chondrules, multiple spot analyses (n=4-10; 10-15 μm in diameter) were performed to test internal homogeneity of O-isotopes.

O-Isotope Homogeneity: Most chondrules have internally homogeneous O-isotopes [27]. In the most primitive carbonaceous (C) chondrite Acfer 094 (ungrouped), multiple mineral phases and glass within a chondrule show indistinguishable O-isotope ratios (Fig. 1, [11]). The exception is a minor occurrence of relict olivine grains with distinct O-isotope ratios, which likely remained solid during the final chondrule melting event due to their relatively high melting temperatures [11-12]. Excluding relict olivine data, host O-isotope ratios of the final chondrule melt are calculated from the mean of only homogeneous data (Fig. 1). The variability of host O-isotope ratios among chondrules is commonly reported as $\Delta^{17}\text{O}$ ($= \delta^{17}\text{O} -$

$0.52 \times \delta^{18}\text{O}$), which is the $\delta^{17}\text{O}$ deviation from the terrestrial fractionation line (TFL; Fig. 1).

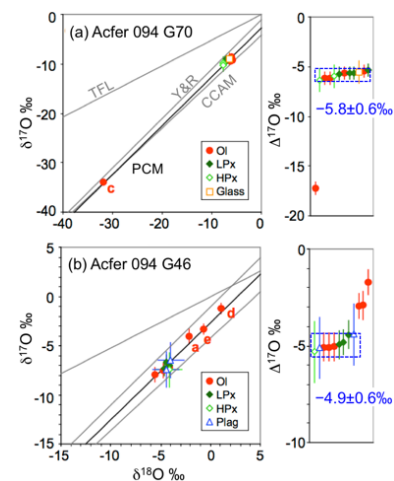


Fig. 1. O-isotope ratios of chondrules in Acfer 094 [11]. Homogeneous data (dashed box) represent those of final melt. Three slope ~1 reference lines (CCAM, Y&R, and PCM) are shown [1,11,28].

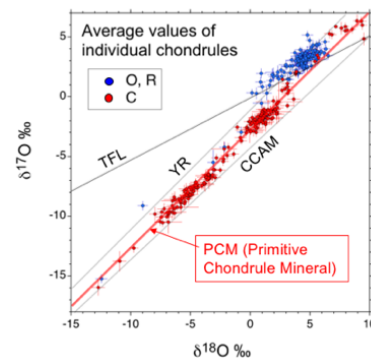


Fig. 2. O-isotope ratios of individual chondrules in O, R, CO, CV, CR, CH, Acfer 094, and Y-82094 ungrouped C chondrites [10-15, 19-21].

General Trend in the O 3-Isotope Diagram:

Chondrules show two distinct trends in O 3-isotope space (Fig. 2). Chondrule data from carbonaceous (C) chondrites plot mainly on the slope ~1.0 primitive chondrule mineral (PCM) line [11], which passes through data from the terrestrial mantle, CAIs and COS. Therefore, the PCM line may represent primary mass independent fractionation of O-isotopes in the protoplanetary disk. Chondrule data from ordinary (O) and Rumurutiite (R) chondrites plot above the TF and PCM lines with a slope of ~0.5, suggesting they experienced mass-dependent isotope fractionation effects

[10, 19-20]. Chondrule data from enstatite (E) chondrites show similar trends to chondrules from O and R chondrite [16]. However, a few chondrules from O, R, and E chondrites also plot below the TF line and on PCM line, similar to those of C chondrite chondrules.

Mg#- $\Delta^{17}\text{O}$ Relationship: FeO contents of chondrule olivine and pyroxene, expressed as Mg# ($[\text{MgO}]/[\text{FeO}+\text{MgO}]$ in mol.%), depend on oxygen fugacity during chondrule formation [e.g., 13] and bulk Fe. Most chondrules in O and R chondrites show slightly positive $\Delta^{17}\text{O}$ values ($\sim 1\text{‰}$) regardless of Mg# [10, 19-20]. The distribution of $\Delta^{17}\text{O}$ values of chondrules in CO and Acfer 094 are bimodal (Fig. 3a); (1) $\text{Mg}\# \geq 98$ and $\Delta^{17}\text{O} \sim -5\text{‰}$ and (2) $\Delta^{17}\text{O} \sim -2.5\text{‰}$ with a wide range of Mg# (99-30) [11-12]. In CR chondrites, the $\Delta^{17}\text{O}$ values of chondrules show a monotonic increase with decreasing Mg# (Fig. 3b), from -6‰ to 0‰ . [13] interpreted this trend as mixing between ^{16}O -rich anhydrous dust ($\Delta^{17}\text{O} = -6\text{‰}$) and ^{16}O -poor water ice ($\Delta^{17}\text{O} = +5\text{‰}$) with dust-enrichments of $\times 100$ -2500.

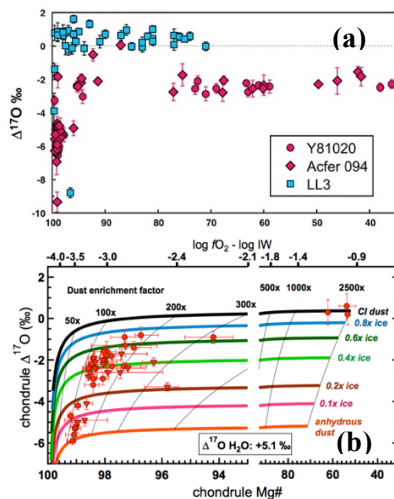


Fig. 3. Mg#- $\Delta^{17}\text{O}$ relationships among chondrules (a) CO (Y-81020), Acfer 094 and O (LL3) [10-12]. (b) CR data with O-isotope mixing model [13].

In CV, CM, and Y-82094, the majority of chondrules are those with highest Mg# (≥ 98) and $\Delta^{17}\text{O} \sim -5\text{‰}$ [14-15, 22-25]. They also contain chondrules with lower Mg#'s and $\Delta^{17}\text{O}$ values of $\sim -2.5\text{‰}$, but are less abundant compared to those in CO and Acfer 094. In addition, a few chondrules in Y-82094 and CV with intermediate Mg# (~ 85) show $\Delta^{17}\text{O} \sim 0\text{‰}$, which are similar to chondrules in O chondrites [14, 23, 26].

The majority of chondrules in CH are high Mg# (90-100) with a $\Delta^{17}\text{O}$ of -2.2‰ [21], similar to those reported for chondrules in CB by [29]. They also contain less abundant chondrules with highest Mg# (≥ 98) and lower $\Delta^{17}\text{O} \sim -6\text{‰}$, as well as those with lower Mg# (90-60) and higher $\Delta^{17}\text{O} \sim +1.5\text{‰}$ [21].

Chondrules in EH and metal-rich ungrouped chondrites (NWA 5492 and GRO 9551) are mostly $\text{Mg}\# > 98$ and have $\Delta^{17}\text{O}$ values of 0 - 1‰ [16-18].

Implication for O Isotope Reservoirs: The Mg# - $\Delta^{17}\text{O}$ systematics among chondrules in C chondrites suggest that they formed near the H_2O ice condensation front (snow line) where precursor solids contained anhydrous dust and water ice with distinct $\Delta^{17}\text{O}$ values. Anhydrous dusts with $\Delta^{17}\text{O} \sim -5\text{‰}$ would have been widely distributed in the protoplanetary disk near the snow line. In contrast, nearly constant and slightly positive $\Delta^{17}\text{O}$ values are observed from a wide range of Mg# among chondrules in O, E, R chondrites. They might have formed at the inner disk regions where O-isotope ratios were significantly homogenized among chondrule precursors, possibly by high temperature heating of the disk that predated chondrule formation.

Each chondrite group shows specific ranges of Mg# and $\Delta^{17}\text{O}$ often with multiple peaks, suggesting each parent asteroid contains multiple populations of chondrules. If they represent chondrules from different regions of the disk, they provide important constraints for radial transport of solids in the disk [30].

References: [1] Clayton R. N. et al. (1977) EPSL, 34, 209-224. [2] McKeegan K. D. et al. (2011) Science, 332, 1528-1532. [3] Sakamoto N. et al. (2007) Science, 317, 231-233. [4] Krot A. N. et al. (2006) Chemie der Erde, 66, 249-276. [5] Kita N. T. and Ushikubo T. (2012) MaPS, 47, 1108-1119. [6] Kita et al. (2013) MaPS, 48, 1383-1400. [7] Ebel D. S. and Grossman L. (2000) GCA, 64, 339-366. [8] Alexander C.M.O'D. et al. (2004) GCA, 68, 3943-3969. [9] Nagahara H. et al. (2008) GCA, 72, 1442-1465. [10] Kita N. T. et al. (2010) GCA, 74, 6610-6635. [11] Ushikubo T. et al. (2012) GCA, 90, 242-264. [12] Tenner T. J. et al. (2013) GCA, 102, 226-245. [13] Tenner T. J. et al. (2015) GCA, 148, 228-250. [14] Tenner T. J. et al. (2017) MaPS, 52, 268-294. [15] Rudraswami N. G. et al. (2011) GCA, 75, 7596-7611. [16] Weisberg M. K. et al. (2011) GCA, 75, 6556-6569. [17] Weisberg M. K. et al. (2015) GCA, 167, 269-285. [18] Weisberg M. K. et al. (2010) LPSC 41, #1756. [19] Kita N. T. et al. (2008) LPSC 39, #2059. [20] Kita N. T. et al. (2015) LPSC 46, #2053. [21] Nakashima D. et al. (2010) MaPS, 47, A148. [22] Hertwig A. et al. (2016) MaPS, 51, #6472. [23] Hertwig A. et al. (2017) LPSC 48, #1227. [24] Chaumard N. et al. (2016) MaPS, 51, #6408. [25] Chaumard N. et al. (2017) LPSC 48, #1610. [26] Defouilloy C. et al. (2016) Goldschmidt Conf. #629. [27] Kita N. T. et al. (2016) LPSC 47, #2375. [28] Young E. D. and Russell S. S. (1998) Science, 282, 452-455. [29] Krot A. N. et al. (2010) GCA, 74, 2190-2211. [30] Cuzzi J. N. et al. (2010) Icarus, 208, 518-538.